Regulatory Mechanisms in Biosystems

ISSN 2519-8521 (Print)
ISSN 2520-2588 (Online)
Regul. Mech. Biosyst.

Immunogenomic stratification of the tumor microenvironment in surgically treated non-small cell lung cancer: A Ukrainian single-center experience

Y. Moskalenko, N. Hyriavenko, T. Derevianko

Sumy State University, Sumy, Ukraine

Article info

Received 16.05.2025
Received in revised form 20.06.2025
Accepted 27.07.2025

Sumy State University, Kharkivska str., 116, Sumy, 40000, Ukraine.
Tel.: +380542334058.
E-mail: yl.moskalenko@med.sumdu.edu.ua

Moskalenko, Y., Hyriavenko, N., & Derevianko, T. (2025). Immunogenomic stratification of the tumor microenvironment in surgically treated non-small cell lung cancer: A Ukrainian single-center experience. Regulatory Mechanisms in Biosystems, 16(3), e25136. doi:10.15421/0225136

Non-small cell lung cancer (NSCLC) remains the leading cause of cancer-related mortality worldwide. Despite radical surgical resection, recurrence is frequent, highlighting the need for improved stratification methods and adjuvant therapeutic strategies. Immunotherapy has demonstrated efficacy in metastatic NSCLC; however, its role in surgically treated patients is still under investigation. This study aimed to analyze the immune landscape of the tumor immune microenvironment in resected NSCLC specimens, identify immune clusters, and evaluate their relationship with patient survival and tumor molecular characteristics. A single-center retrospective study was conducted on 42 patients with stage I–IIIB NSCLC who underwent surgical resection between 2015 and 2018. All patients received platinum-based adjuvant chemotherapy; 35.7% received additional atezolizumab immunotherapy, and 11.9% received adjuvant radiotherapy. Tumor samples were assessed via immunohistochemistry for $CD8^+$ cytotoxic T cells, $FoxP3^+$ regulatory T cells, $CD68^+$ (M1), and $CD163^+$ (M2) macrophages in both tumor islets and stroma. Expression levels were stratified into high/low groups based on validated cut-offs. PD-L1 status was also evaluated. Seven immune markers were analyzed using principal component analysis and k-means clustering (k = 2) to define immune phenotypes. Next-generation sequencing was performed using the AmoyDx Essential Panel targeting ten major driver mutations. Survival was assessed using Kaplan-Meier estimates and log-rank tests. Two distinct immune phenotypes were identified: an immunoactive cluster (n = 14) with high $CD8^+$ and M1 infiltration, and an immunosuppressive cluster (n = 28) characterized by increased $FoxP3^+$ and M2 expression. Although not statistically significant, the immunoactive group showed a trend toward improved outcomes: median progression-free survival was 98.8 in the immunoactive cluster vs. 27.8 months (P = 0.543) in the immunosuppressive cluster, and overall survival was 114.5 in the immunoactive cluster vs. 38.1 months (P = 0.435) in the immunosuppressive cluster. NGS revealed mutations in 26.2% of tumor samples (KRAS 16.7%, EGFR 4.8%, ALK 2.4%, BRAF 2.4%), with no significant difference between clusters (P = 0.810), suggesting independence between molecular and immune profiles. In conclusion, immune-based stratification identified distinct TME phenotypes associated with survival trends in surgically treated NSCLC. Integrating immunohistochemistry and next-generation sequencing may improve personalized adjuvant treatment selection. Larger studies are needed to validate these findings.

Keywords: tumor immune microenvironment; next-generation sequencing; non-small cell lung cancer; $CD8^+$; $FoxP3^+$; $CD68^+$; $CD163^+$.

Introduction

Non-small cell lung cancer (NSCLC) accounts for over 85% of all lung cancer cases and remains the leading cause of cancer-related mortality worldwide (De Lucia et al., 2025; Tang et al., 2025). Despite notable advancements in screening methods such as low-dose computed tomography (LDCT), early-stage diagnosis continues to be relatively uncommon, largely due to the asymptomatic nature of the disease in its initial stages and limited access to high-quality diagnostic tools in many regions. As a result, a substantial proportion of patients are still diagnosed at advanced stages when curative treatment options are limited (Tang et al., 2025).

Even after radical surgical resection in early-stage disease, the risk of recurrence remains high, with recurrence-free survival (RFS) strongly influenced by pathological stage, lymphovascular invasion, and molecular features (Rajaram et al., 2024). This underscores the persistent need for effective and individualized adjuvant treatment strategies that can improve long-term survival outcomes. While platinum-based chemotherapy remains a mainstay, recent research suggests that integrating molecular profiling and immune characterization could guide more precise interventions (Nagasaka et al., 2023; Lieber et al., 2024).

In this context, immunotherapy – particularly immune checkpoint inhibitors (ICIs) – has ushered in a new era in the management of NSCLC. PD-1/PD-L1 inhibitors such as pembrolizumab and atezolizumab have demonstrated considerable efficacy in patients with metastatic disease. However, their role in the adjuvant setting following surgery is still being defined. Clinical trials such as IMpower010 and PEARLS/KEYNOTE-091 have yielded mixed results, with differences depending on PD-L1 expression thresholds, mutational status, and prior chemotherapy use (Girard et al., 2023; Lieber et al., 2024). For example, Girard (2023) emphasizes the need for high PD-L1 expression (≥50%) as a potential condition for adjuvant immunotherapy benefit, indicating the importance of precise patient selection.

One of the major limitations of immunotherapy in early-stage NSCLC is the heterogeneity of the tumor microenvironment (TME), which significantly influences therapeutic response (Casanova-Acebes et al., 2021; Chandra et al., 2025). The TME consists of a complex interplay of immune and stromal elements, including T lymphocytes, macrophages, dendritic cells, fibroblasts, endothelial cells, and extracellular matrix components (Duan et al., 2022). Importantly, the immunological features of this milieu – such as the density of $CD8^+$ cytotoxic T cells, macrophage polarization into tumor-promoting M2 versus tumor-inhibiting M1 phenotypes, and the prevalence of regulatory T cells ($FoxP3^+$) – have been closely associated with disease prognosis and immunotherapeutic efficacy (Zhang et al., 2021; Gurevičienė et al., 2024).

For instance, high infiltration of $CD8^+$ T cells typically correlate with better prognosis and heightened response to ICIs, while an immune landscape dominated by $FoxP3^+$ regulatory T cells or M2 macrophages creates an immunosuppressive niche that may impair antitumor immunity (Toki et al., 2018; Sellmer et al., 2022). This highlights the necessity of moving beyond a simplistic biomarker approach based solely on PD-L1 expression, and toward more nuanced stratification using comprehensive immune profiles (Boscolo et al., 2020). Kanemura et al. (2024) have further shown that immune infil-

tration patterns within early-stage lung adenocarcinoma correlate with recurrence risk, suggesting potential utility for immune-based prognostic tools. Furthermore, modern statistical and computational approaches – including principal component analysis, clustering algorithms, and unsupervised machine learning techniques – have begun to reveal hidden immune phenotypes and facilitate objective classification of TME subtypes (Teshima et al., 2022; Gaiffe et al., 2023). These data-driven classifications may guide the development of tailored immunotherapeutic strategies and serve as the foundation for precision oncology in NSCLC.

To the best of our knowledge, this is the first study conducted in Ukraine to simultaneously perform extended immunohistochemical profiling of the tumor immune microenvironment and next-generation sequencing (NGS) analysis in surgically treated NSCLC patients. By integrating immune phenotyping with molecular and clinical outcome data, this research aims to establish a localized yet relevant foundation for precision medicine, potentially informing future therapeutic decisions in the Ukrainian oncological context. This study hypothesizes that the immune phenotype of the TME is associated with survival outcomes and the molecular profile of tumors in surgically treated NSCLC patients. The objective was to analyze the immune landscape of the TME in resected NSCLC specimens, identify immune clusters, and evaluate their relationship with patient survival and tumor molecular characteristics.

Materials and methods

Study design and ethics approval. The research was carried out in compliance with the principles of medical ethics and the protection of patients rights, human dignity and moral and ethical norms, in accordance with the principles of the Helsinki Declaration of Human Rights, the Council of Europe Convention on Human Rights and Biomedicine, and the laws of Ukraine. The study was approved by the Bioethics Committee of Sumy State University (protocol No. 3/12, dated 17.12.2024). All patients alive at the start of the study provided written informed consent.

This study included 42 patients aged over 18 years diagnosed with stage I–IIIB NSCLC, who underwent surgical resection and received adjuvant therapy between 2015 and 2018 in accordance with clinical indications. All patients received 2 to 4 cycles of platinum-based chemotherapy following the National Comprehensive Cancer Network (NCCN) guidelines. In selected cases, the treatment regimen was supplemented with immunotherapy using atezolizumab (1200 mg intravenously every 21 days) for up to one year or until disease progression. Additionally, radiotherapy was administered in cases with N_2 lymph node involvement.

The study did not aim to compare the efficacy of different therapeutic approaches; therefore, treatment type was not used as a stratification variable in the primary analysis. The main focus was to investigate the association between the immune phenotype of the TME and survival outcomes. Clinicopathological data – including patient age, sex, disease stage, and tumor histological subtype – were collected from medical records and summarized in tables. Exclusion criteria included the use of neoadjuvant chemotherapy or radiotherapy, the presence of severe comorbidities (e.g., decompensated diabetes mellitus, advanced heart failure, or uncontrolled hypertension with high cardiovascular risk), and stage IV NSCLC.

Immunohistochemical analysis of the TME. The density of immune cell infiltration in tumor tissue samples was assessed using immunohistochemistry. The following markers were evaluated: regulatory T cells ($FoxP3^+$), cytotoxic $CD8^+$ T cells, M1 macrophages ($CD68^+$), and M2 macrophages ($CD163^+$), both in stroma and tumor islets. NSCLC tissue samples were cut into serial sections 4 μm thick and mounted onto SuperFrost adhesive slides (Thermo Scientific, USA). Slides were dried at 60 °C for 18 hours. Deparaffinized sections underwent heat-induced epitope retrieval in 0.1 M citrate buffer (pH 6.0) at 95–98 °C for 20 minutes, followed by cooling to room temperature and triple rinsing with distilled water. Endogenous peroxidase activity was blocked using a commercial reagent (MAD-021540Q-125) for 10 minutes. Sections were then incubated with primary monoclonal antibodies for 10 minutes, and staining was visualized using the *in vitro* detection system (Master-Diagnostica, Granada, Spain). For each marker, six high-density areas of positive immune cell infiltration (1 mm² each) were selected per sample, and average values were calculated. To detect regulatory T cells, rabbit monoclonal antibodies against the transcription factor $FoxP3^+$ (clone EP340, Cell Marque, Rocklin, CA, USA, 2023) were applied. The threshold for $FoxP3^+$ expression was set at 23 cells/mm². Based on this, patients were classified into low (<23 cells/mm²) and high (≥23 cells/mm²) $FoxP3^+$ infiltration groups. Tumor-associated macrophages were visualized using mouse monoclonal anti-$CD68^+$ antibodies (Clone KP-1, Master-Diagnostica, Granada, Spain, 2024) and rabbit anti-$CD163^+$ antibodies (Clone EP324, Master-Diagnostica, Granada, Spain, 2024). All reagents were ready-to-use. Expression thresholds were defined by mean values: M1 macrophages – 18 cells/mm² in tumor tumour islets, 11 cells/mm² in stroma; M2 macrophages – 13 cells/mm² in tumour islets, 24 cells/mm² in stroma. Cytotoxic T cells ($CD8^+$) were detected using monoclonal antibodies (clone C8/144B, Dako, Glostrup, Denmark, 2023). Stratification thresholds for $CD8^+$ expression were: <9 cells/mm² for low tumour islets infiltration, <24 cells/mm² for low stromal infiltration. PD-L1 expression was assessed using monoclonal antibodies (Clone Cal-10, Master Diagnostica; dilution 1:50). Based on PD-L1 expression, tumor samples were stratified into three groups: <1%, 1–49%, and ≥50%. A reaction was considered positive if a distinct membranous staining of NSCLC tumor cells was observed, possibly accompanied by partial or full cytoplasmic staining of variable intensity. Staining of tumor-associated immune cells (e.g., macrophages and lymphocytes), as well as cytoplasmic-only reactivity, was not included in the assessment. All IHC evaluations were performed by a qualified pathologist.

Survival analysis. Survival time was measured in months from the date of surgical resection to the occurrence of an event (disease progression or death) or the last follow-up. The final analysis of progression-free survival and overall survival was performed as of June 1, 2025. Mortality data were collected through the Cancer Registry of the Sumy Regional Clinical Oncology Center.

Next-generation sequencing analysis. To assess the molecular profile of tumor tissue, NGS was conducted. DNA was extracted from formalin-fixed paraffin-embedded blocks using the E.Z.N.A.® FFPE DNA Kit (Omega Bio-tek, USA), following the manufacturer's instructions. DNA concentration was measured using the dsDNA Broad Range Assay (DeNovix, USA), and DNA integrity was evaluated using the PreSeq DNA QC Assay (ArcherDX, USA). Targeted sequencing was performed using the AmoyDx Essential NGS Panel (AmoyDx, China), which covers key driver mutations relevant to NSCLC. Library preparation followed the manufacturer's protocol, using a minimum of 30 ng of DNA per reaction. Libraries were quantified using the KAPA Library Quantification Kit (Roche, Switzerland), and fragment sizes were checked using the Agilent TapeStation system (Agilent Technologies, USA). Libraries were normalized to 4 nM, pooled, and sequenced on the Illumina NextSeq 550Dx platform (USA) with the NextSeq 550 Mid-Output Kit. Data processing, variant annotation, and classification were performed using the ANDAS ADXLC10 platform (version 3.3.0, AmoyDx).

Statistical analysis. Statistical analysis was conducted using Stata software version 19.5 (StataCorp, Texas, USA; www.stata.com, 2025). Clinicopathological characteristics were presented as absolute numbers and percentages. For the variable "age", mean ± standard deviation was reported. PFS and OS were estimated using the Kaplan-Meier method, and differences between survival curves were tested using the log-rank test. A p-value <0.05 was considered statistically significant. To stratify patients based on the immune phenotype of the tumor TME, principal component analysis followed by k-means clustering was performed. Seven immune variables were included in the PCA: stromal $CD8^+$, intra-tumoral $CD8^+$, $FoxP3^+$, stromal $CD68^+$, intra-tumoral $CD68^+$, stromal $CD163^+$, and intra-tumoral $CD163^+$. All values were standardized (Z-scores) prior to principal component analysis and clustering. The principal component analysis reduced the dimensionality of the data to two principal components.

The first principal component represented an immunoactivity gradient, with high loadings for $CD8^+$ T cells and M1 macrophages. The second component differentiated samples based on the presence of regulatory T cells and M2 macrophages. Subsequently, k-means clustering (k = 2) was applied. Patients were divided into two clusters: an immunoactive cluster (n = 14) and an immunosuppressive cluster (n = 28). The immunoactive group was characterized by high densities of $CD8^+$ T cells and M1 macrophages in both tumor islands and stroma, and low expression of $FoxP3^+$ and M2 macrophages. The immunosuppressive cluster included patients with low $CD8^+$ and M1 cell densities and high expression of $FoxP3^+$ and M2 macrophages in both compartments. Principal component analysis results were visualized using a scatterplot.

Results

Clinicopathological characteristics of the study population. A total of 42 patients with resected NSCLC were included. The mean age was 58.5 ± 8.5 years; most patients were male (81.0%) and younger than 60 years (52.4%). Histologically, squamous cell carcinoma was the most prevalent subtype (52.4%). All patients received adjuvant chemotherapy, and 35.7% additionally received immunotherapy. Radiotherapy was administered in 11.9% of cases.

Immunohistochemistry analysis revealed high $CD8^+$ T-cell infiltration in tumor islets in 69% of cases and in the stroma in 52.4%. High $FoxP3^+$ regulatory T-cell expression was found in 57.1% of patients. High M1 macrophages expression was predominated in tumor islets (61.9%). High M2 macrophage expression was observed in stroma of 50.0% of samples and in islets of 35.7% of samples. Next-generation sequencing-based molecular analysis showed low frequencies of driver mutations: EGFR mutations were detected in 4.8% of patients, ALK in 2.4%, BRAF in 2.4%, and KRAS in 16.7% (Table 1).

Tumor microenvironment clustering. Based on principal component analysis and k-means clustering, two immunologically distinct TME phenotypes were identified: an immunoactive cluster (n = 14) and an immunosuppressive cluster (n = 28). Figure 1 illustrates the distribution of patients in the space of the first two principal components, demonstrating a clear separation between the clusters. Patients in the immunoactive cluster were concentrated within a specific region of the plot, while those in the immunosuppressive cluster formed a separate grouping, indicating distinct immune infiltration patterns between the two subgroups.

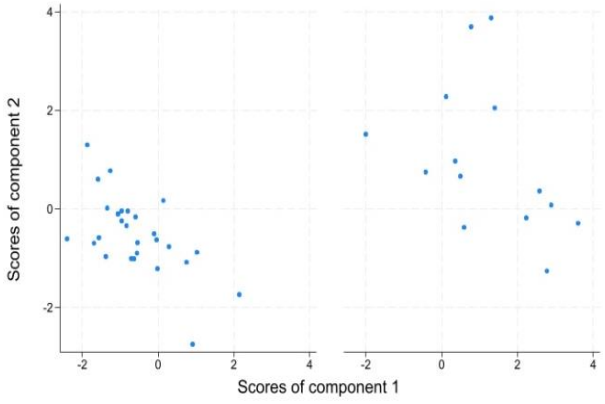

Fig. 1. Distribution of NSCLC patients in the space of the principal components based on tumor microenvironment characteristics: patients were classified into two clusters: an immunosuppressive cluster (*a*) and an immunoactive cluster (*b*), based on the density of $CD8^+$ T cells, M1/M2 macrophages, and $FoxP3^+$ regulatory T cells (n = 42)

Thus, principal component analysis combined with clustering revealed two clearly differentiated immune phenotypes among NSCLC patients, which may have both prognostic and predictive relevance in the context of immunotherapy response.

Survival assessment. To evaluate the prognostic relevance of tumor microenvironment clusters, progression-free survival was analyzed using the Kaplan-Meier method. Survival outcomes were compared between patients from the two clusters defined by immune profiling. The median progression-free survival was 98.8 months in the immunoactive cluster versus 27.8 months in the immunosuppressive cluster; however, this difference did not reach statistical significance (log-rank test: $\chi^2 = 0.37$; P = 0.5433; Fig. 2).

Table 1
Clinicopathological characteristics and tumor microenvironment features in patients with resected NSCLC (n = 42)

Clinicopathological characteristics	Patients with NSCLC, n	Patients with NSCLC, %
Age of patients:		
Medium	58.5 ± 8.5	–
< 60	22	52.4
≥ 60	20	47.6
Sex of patients:		
Female	8	19.0
Male	34	81.0
Tumour histology:		
Adenocarcinoma	20	47.6
Squamous cell carcinoma	22	52.4
Stage of NSCLC:		
IA–IIA	15	35.7
IIB–IIIB	27	64.3
Adjuvant therapy:		
Chemotherapy	27	64.3
Chemoimmunotherapy	15	35.7
Radiation therapy:		
Yes	5	11.9
No	37	88.1
PD-L expression:		
<1 %	12	28.6
1–49 %	24	57.1
≥50	6	14.3
Cytotoxic T cells ($CD8^+$) in tumor islets:		
Low expression	13	30.1
High expression	29	69.0
Cytotoxic T cells ($CD8^+$) in tumor stroma:		
Low expression	20	47.6
High expression	22	52.4
Regulatory T-cells ($FoxP3^+$):		
Low expression	18	42.9
Hight expression	24	57.1
Macrophages M1 ($CD68^+$) in tumor islets:		
Low expression	16	38.1
High expression	26	61.9
Macrophages M1 ($CD68^+$) in tumor stroma:		
High expression	18	42.9
Low expression	24	57.1
Macrophages M2 ($CD163^+$) in tumor islets:		
High expression	15	35.7
Low expression	27	64.3
Macrophages M2 ($CD163^+$) in tumor stroma:	21	50.0
High expression	21	50.0
Low expression		
EGFR mutation:		
Absent	40	95.2
Present	2	4.8
ALK mutation:		
Absent	41	97.6
Present	1	2.4
BRAF mutation:		
Absent	41	97.6
Present	1	2.4
KRAS mutation:		
Absent	35	83.3
Present	7	16.7

An additional analysis of overall survival was conducted among surgically treated NSCLC patients, stratified by tumor microenvironment cluster. Patients in the immunoactive cluster exhibited a longer median overall survival (114.5 months) compared to those in the im-

munosuppressive cluster (38.1 months). However, this difference did not reach statistical significance according to the log-rank test (χ^2 = 0.61; p = 0.4354; Fig. 3).

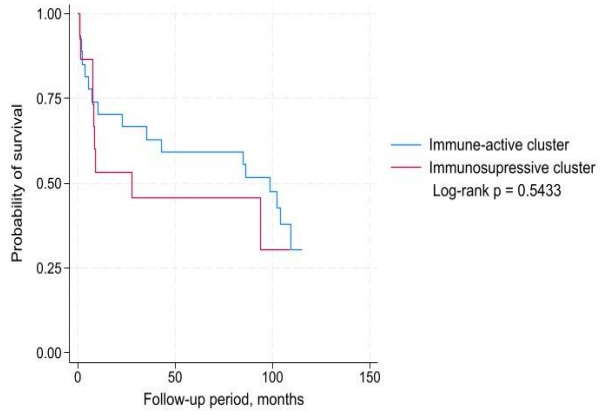

Fig. 2. Progression-free survival in surgically treated NSCLC patients according to tumor microenvironment cluster affiliation (n = 42)

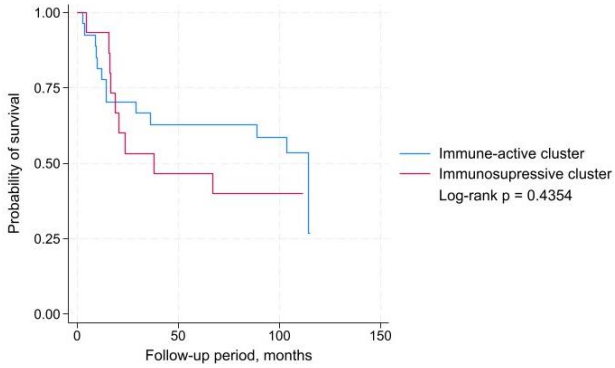

Fig. 3. Overall survival in surgically treated NSCLC patients according to tumor microenvironment cluster classification (n = 42)

The results indicate a trend toward prolonged disease control among patients with an immunoactive tumor microenvironment. However, the lack of statistical significance is likely attributable to the limited sample size and number of events.

Molecular profiling. Next-generation sequencing identified a total of 11 mutations across 42 NSCLC tumor samples. In the immune-active cluster (n = 14), three patients (21.4%) harbored oncogenic variants. These included one EGFR Leu858Arg mutation (c.2573T>G), one KRAS G12C substitution (c.34G>T), and one KRAS A146S alteration (c.436G>T).

Among patients in the immunosuppressive cluster (n = 28), eight individuals (28.6%) exhibited mutations. This group included one case of EGFR Leu858Arg, one ALK rearrangement (EML4–ALK translocation between exon 6 and exon 20; chromosomal coordinates chr2:42503838–29447579), and six KRAS mutations: two G12C (c.34G>T), one G12A (c.35G>C), and two G12D (c.35G>A). Additionally, a single case of BRAF V600E (c.1799T>A) was detected in the immunosuppressive group.

No mutations were identified in ROS1, NRAS, RET, ERBB2, MET, or PIK3CA in either cluster. The overall mutation frequency did not significantly differ between the immune phenotypes (21.4% vs. 28.6%; P = 0.8099), suggesting that immune microenvironment profiles may be independent of common oncogenic driver alterations.

Discussion

The results of this study confirm the presence of two phenotypically distinct immune patterns in the TME of NSCLC patients following surgical treatment. The immunoactive phenotype was associated with a higher density of $CD8^+$ T cells and M1 macrophages, while the immunosuppressive phenotype was characterized by an abundance of $FoxP3^+$ regulatory T cells and M2 macrophages. Similar immunological features have been described in the literature as potential predictors of response to immunotherapy (Pirlog et al., 2022; Gurevičienė et al., 2024). Tuminello et al. (2021) demonstrated that a high density of $CD8^+$ T cells in the early-stage NSCLC TME was associated with improved progression-free survival, increasing median progression-free survival from 32 to over 60 months. In our study, patients with an immunoactive TME exhibited a median overall survival of 114.5 months compared to 38.1 months in those with an immunosuppressive TME. However, this difference did not reach statistical significance, likely due to the limited sample size. Similarly, the median progression-free survival was 98.8 months in the immunoactive cluster versus 27.8 months in the immunosuppressive cluster (P = 0.543). This trend is consistent with analyses by Abdelfatah et al. (2023), which showed that the presence of $CX3CR1^+$ $CD8^+$ T cells in NSCLC patients after chemoimmunotherapy was linked to improved survival. Interestingly, clinicopathological characteristics such as age, sex, disease stage, and histological subtype did not differ significantly between the clusters. This highlights the pivotal role of TME immune profiling in risk stratification and therapeutic decision-making. Such a shift in focus from conventional morphology and staging toward immune classification is gaining momentum in current oncology literature (Yang et al., 2023).

The integration of next-generation sequencing added depth to our understanding of the molecular landscape. Mutation analysis revealed no significant differences in the frequency of EGFR, ALK, KRAS, and BRAF mutations between immune clusters. This finding aligns with data from Hu et al. (2021) and Pop-Bica et al. (2022), who report that mutational status does not necessarily correlate with the tumor's immune context. Meanwhile, Yadav et al. (2023) emphasize that NGS is transforming precision oncology by enabling the detection of rare driver mutations, tumor burden, and potential immunotherapy responsiveness.

Our finding of no association between mutation status and immune phenotype echoes the conclusions of Guo et al. (2021), who noted that PD-L1 expression, mutational burden, and mutation profiles do not always correlate with $CD8^+$ T-cell infiltration. This issue gains further importance in light of data from Zhang et al. (2024), who identified substantial heterogeneity in PD-L1 expression and tumor mutational burden between primary tumors and metastases. Hence, PD-L1 alone may not adequately reflect the complexity of tumor–immune interactions.

Stratification based on immune phenotype may have direct clinical utility. Federico et al. (2022) and Kanemura et al. (2024) demonstrate that combining spatial cell distribution with molecular markers improves recurrence prediction after surgery. In our study, spatial organization was considered through separate analyses of immune cell infiltration in both tumor islets and stroma, allowing a more accurate depiction of the functional immune landscape. This methodological strength reflects the real dynamics between tumor cells and the immune system. The immunoactive cluster was clearly marked by high infiltration of $CD8^+$ and M1 cells, which has been previously shown by Sellmer et al. (2022) as a predictor of favorable prognosis in early-stage NSCLC. Conversely, Dell'Amore et al. (2023) argue that in early adenocarcinoma, the TME may not always serve as an independent prognostic factor. This contrast in findings underscores the heterogeneity of the TME and the need for multifactorial assessments – an area being actively explored with artificial intelligence, as illustrated by Terada et al. (2023).

The practical implications of our findings are multifaceted. Implementing multi-parameter immune stratification may not only improve prognosis estimation but also guide therapy adaptation, especially in the context of high-cost immunotherapy (Escudero-Vilaplana et al., 2023). As Li MSC et al. (2023) aptly noted, the integration of immune and molecular biomarkers represents the path toward truly personalized oncology.

Nevertheless, several limitations must be acknowledged. First, the modest sample size (n = 42) precludes definitive statistical conclusions. Second, the retrospective design introduces the possibility of selection bias. Given the limited number of patients who received immunotherapy, we refrained from comparing treatment-specific outcomes. The aim of this study was not to assess the efficacy of particular

treatment regimens, but rather to investigate the prognostic significance of TME immune profiles. A promising direction for future research includes prospective, multi-center studies that incorporate molecular and immunological validation of the clustering model.

Conclusions

This study demonstrates that the immune phenotype of the tumor microenvironment – particularly the balance of $CD8^+$ T cells, M1/M2 macrophages, and $FoxP3^+$ regulatory T cells in tumor islets and stroma – may hold prognostic and predictive value in surgically treated NSCLC patients. Two distinct immune clusters were identified, differing in both morphological characteristics and survival trends. Although differences in overall survival and progression-free survival were not statistically significant, patients with an immunoactive profile showed a tendency toward improved outcomes. Thus, stratification by immune phenotype holds potential for enhancing adjuvant treatment decisions and identifying candidates for immunotherapy post-surgery. Future studies are needed to validate these findings in larger cohorts with prospective, multicenter data.

This research has been performed with the financial support of grants of the external aid instrument of the European Union for the fulfillment of Ukraine's obligations in the Framework Program of the European Union for Scientific Research and Innovation "Horizon 2020" No. RN/ 11 – 2023 "The role of the DNA repair system in the pathogenesis and immunogenicity of lung cancer".

The authors declare no conflict of interest.

References

Abdelfatah, E., Long, M. D., Kajihara, R., Oba, T., Yamauchi, T., Chen, H., Sarkar, J., Attwood, K., Matsuzaki, J., Segal, B. H., Dy, G. K., & Ito, F. (2023). Predictive and prognostic implications of circulating CX3CR1+ CD8+ T cells in non-small cell lung cancer patients treated with chemoimmunotherapy. Cancer Research Communications, 3(3), 510–520.

Boscolo, A., Fortarezza, F., Lunardi, F., Comacchio, G., Urso, L., Frega, S., Menis, J., Bonanno, L., Guarneri, V., Rea, F., Conte, P., Calabrese, F., & Pasello, G. (2020). Combined immunoscore for prognostic stratification of early stage non-small-cell lung cancer. Frontiers in Oncology, 10, 564915.

Casanova-Acebes, M., Dalla, E., Leader, A. M., LeBerichel, J., Nikolic, J., Morales, B. M., Brown, M., Chang, C., Troncoso, L., Chen, S. T., Sastre-Perona, A., Park, M. D., Tabachnikova, A., Dhainaut, M., Hamon, P., Maier, B., Sawai, C. M., Agulló-Pascual, E., Schober, M., Brown, B. D., & Merad, M. (2021). Tissue-resident macrophages provide a pro-tumorigenic niche to early NSCLC cells. Nature, 595(7868), 578–584.

Chandra, R., Ehab, J., Hauptmann, E., Gunturu, N. S., Karalis, J. D., Kent, D. O., Heid, C. A., Reznik, S. I., Sarkaria, I. S., Huang, H., Brekken, R. A., Minna, J. D. (2025). The current state of tumor microenvironment-specific therapies for non-small cell lung cancer. Cancers, 17(11), 1732.

De Lucia, A., Mazzotti, L., Gaimari, A., Zurlo, M., Maltoni, R., Cerchione, C., Bravaccini, S., Delmonte, A., Crinò, L., Borges de Souza, P., Pasini, L., Nicolini, F., Bianchi, F., Juan, M., Calderon, H., Magnoni, C., Gazzola, L., Ulivi, P., & Mazza, M. (2025). Non-small cell lung cancer and the tumor microenvironment: Making headway from targeted therapies to advanced immunotherapy. Frontiers in Immunology, 16, 1515748.

Duan, J., Lv, G., Zhu, N., Chen, X., Shao, Y., Liu, Y., Zhao, W., & Shi, Y. (2022). Multidimensional profiling depicts infiltrating immune cell heterogeneity in the tumor microenvironment of stage IA non-small cell lung cancer. Thoracic Cancer, 13(7), 947–955.

Escudero-Vilaplana, V., Collado-Borrell, R., De Castro, J., Insa, A., Martínez, A., Fernández, E., Sullivan, I., Flores, A., Arrabal, N., Carcedo, D., & Manzaneque, A. (2023). Cost-effectiveness of adjuvant atezolizumab versus best supportive care in the treatment of patients with resectable early-stage non-small cell lung cancer and overexpression of PD-L1. Journal of Medical Economics, 26(1), 445–453.

Federico, L., McGrail, D. J., Bentebibel, S. E., Haymaker, C., Ravelli, A., Forget, M. A., Karpinets, T., Jiang, P., Reuben, A., Negrao, M. V., Li, J., Khairullah, R., Zhang, J., Weissferdt, A., Vaporciyan, A. A., Antonoff, M. B., Walsh, G., Lin, S. Y., Futreal, A., Wistuba, I., & Bernatchez, C. (2022). Distinct tumor-infiltrating lymphocyte landscapes are associated with clinical outcomes in localized non-small-cell lung cancer. Annals of Oncology, 33(1), 42–56.

Gaiffe, E., Colladant, M., Desmaret, M., Bamoulid, J., Leroux, F., Laheurte, C., Brouard, S., Giral, M., Saas, P., Courivaud, C., Degauque, N., & Ducloux, D. (2023). Pre-transplant immune profile defined by principal component analysis predicts acute rejection after kidney transplantation. Frontiers in Immunology, 14, 1192440.

Girard, N. (2023). In patients with early stage NSCLC without driver mutation after surgical resection and chemotherapy: Adjuvant Atezolizumab should only be given for patients with programmed death-ligand 1 greater than or equal to 50. Journal of Thoracic Oncology, 18(3), 268–270.

Guo, G., Li, G., Liu, Y., Li, H., Guo, Q., Liu, J., Yang, X., Shou, T., & Shi, Y. (2021). Next-generation sequencing reveals high uncommon EGFR mutations and tumour mutation burden in a subgroup of lung cancer patients. Frontiers in Oncology, 11, 621422.

Gurevičienė, G., Matulionė, J., Poškienė, L., Miliauskas, S., & Žemaitis, M. (2024). PD-L1+ lymphocytes are associated with CD4+, Foxp3+CD4+, IL17+CD4+ T cells and subtypes of macrophages in resected early-stage non-small cell lung cancer. International Journal of Molecular Sciences, 25(19), 10827.

Gurevičienė, G., Matulionė, J., Poškienė, L., Miliauskas, S., & Žemaitis, M. (2024). PD-L1 expression and tumour microenvironment patterns in resected non-small-cell lung cancer. Medicina, 60(3), 482.

Hu, C., Zhao, L., Liu, W., Fan, S., Liu, J., Liu, Y., Liu, X., Shu, L., Liu, X., Liu, P., Deng, C., Qiu, Z., Chen, C., Jiang, Y., Liang, Q., Yang, L., Shao, Y., He, Q., Yu, D., Zeng, Y., & Wu, F. (2021). Genomic profiles and their associations with TMB, PD-L1 expression, and immune cell infiltration landscapes in synchronous multiple primary lung cancers. Journal for Immunotherapy of Cancer, 9(12), e003773.

Kanemura, H., Yokoyama, T., Nakajima, R., Nakamura, A., Kuroda, H., Kitamura, Y., Shoda, H., Mamesaya, N., Miyata, Y., Okamoto, T., Okishio, K., Oki, M., Sakairi, Y., Chen-Yoshikawa, T. F., Aoki, T., Ohira, T., Matsumoto, I., Ueno, K., Miyazaki, T., Matsuguma, H., & Takeda, M. (2024). The tumor immune microenvironment is associated with recurrence in early-stage lung adenocarcinoma. Journal of Thoracic Oncology Clinical and Research Reports, 5(4), 100658.

Li, M. S. C., Mok, K. K. S., & Mok, T. S. K. (2023). Developments in targeted therapy and immunotherapy-how non-small cell lung cancer management will change in the next decade: A narrative review. Annals of Translational Medicine, 11(10), 358.

Lieber, A., Makai, A., Orosz, Z., Kardos, T., Isaac, S. J., Tornyi, I., & Bittner, N. (2024). The role of immunotherapy in early-stage and metastatic NSCLC. Pathology Oncology Research, 30, 1611713.

Nagasaka, M., & Ou, S. I. (2023). Stage as the sole "Biomarker" for adjuvant Pembrolizumab in resected stage IB to IIIA NSCLC without considerateons for PD-L1 expression level, ALK/EGFR mutational status, and prior adjuvant chemotherapy per FDA approval indications of PEARLS/ Keynote-091? Lung Cancer, 14, 101–109.

Pirlog, R., Chiroi, P., Rusu, I., Jurj, A. M., Budisan, L., Pop-Bica, C., Braicu, C., Crisan, D., Sabourin, J. C., & Berindan-Neagoe, I. (2022). Cellular and molecular profiling of tumor microenvironment and early-stage lung cancer. International Journal of Molecular Sciences, 23(10), 5346.

Pop-Bica, C., Ciocan, C. A., Braicu, C., Haranguș, A., Simon, M., Nutu, A., Pop, L. A., Slaby, O., Atanasov, A. G., Pirlog, R., Al Hajjar, N., & Berindan-Neagoe, I. (2022). Next-generation sequencing in lung cancer patients: A comparative approach in NSCLC and SCLC mutational landscapes. Journal of Personalized Medicine, 12(3), 453.

Rajaram, R., Huang, Q., Li, R. Z., Chandran, U., Zhang, Y., Amos, T. B., Wright, G. W. J., Ferko, N. C., & Kalsekar, I. (2024). Recurrence-free survival in patients with surgically resected non-small cell lung cancer: A systematic literature review and meta-analysis. Chest, 165(5), 1260–1270.

Sellmer, L., Kovács, J., Walter, J., Kumbrink, J., Neumann, J., Kauffmann-Guerrero, D., Kiefl, R., Schneider, C., Jung, A., Behr, J., & Tufman, A. (2022). Markers of immune cell exhaustion as predictor of survival in surgically-treated early-stage NSCLC. Frontiers in Immunology, 13, 858212.

Tang, F. H., Wong, H. Y. T., Tsang, P. S. W., Yau, M., Tam, S. Y., Law, L., Yau, K., Wong, J., Farah, F. H. M., & Wong, J. (2025). Recent advancements in lung cancer research: a narrative review. Translational Lung Cancer Research, 14(3), 975–990.

Terada, Y., Isaka, M., Ono, A., Kawata, T., Serizawa, M., Mori, K., Muramatsu, K., Tone, K., Kenmotsu, H., Ohshima, K., Urakami, K., Nagashima, T., Kusuhara, M., Akiyama, Y., Sugino, T., Takahashi, T., & Ohde, Y. (2023). Prognostic significance of tumor microenvironment assessed by machine learning algorithm in surgically resected non-small cell lung cancer. Cancer Reports, 2023, e1926.

Teshima, T., Kobayashi, Y., Kawai, T., Kushihara, Y., Nagaoka, K., Miyakawa, J., Akiyama, Y., Yamada, Y., Sato, Y., Yamada, D., Tanaka, N., Tsunoda, T., Kume, H., & Kakimi, K. (2022). Principal component analysis of early immune cell dynamics during pembrolizumab treatment of advanced urothelial carcinoma. Oncology Letters, 24(2), 265.

Toki, M. I., Mani, N., Smithy, J. W., Liu, Y., Altan, M., Wasserman, B., Tuktamyshov, R., Schalper, K., Syrigos, K. N., & Rimm, D. L. (2018). Immune marker profiling and programmed death ligand 1 expression across NSCLC mutations. Journal of Thoracic Oncology, 13(12), 1884–1896.

Tuminello, S., Petralia, F., Veluswamy, R., Wang, P., Flores, R., & Taioli, E. (2021). Prognostic value of the tumor immune microenvironment for early-stage, non-small cell lung cancer. American Journal of Clinical Oncology, 44(7), 350–355.
Yadav, D., Patil-Takbhate, B., Khandagale, A., Bhawalkar, J., Tripathy, S., & Khopkar-Kale, P. (2023). Next-Generation sequencing transforming clinical practice and precision medicine. Clinica Chimica Acta, 551, 117568.
Yang, L., Zhang, W., Sun, J., Yang, G., Cai, S., Sun, F., Xing, L., & Sun, X. (2023). Functional status and spatial interaction of T cell subsets driven by specific tumor microenvironment correlate with recurrence of non-small cell lung cancer. Frontiers in Immunology, 13, 1022638.
Zhang, H., Wang, S. Q., Hang, L., Zhang, C. F., Wang, L., Duan, C. J., Cheng, Y. D., Wu, D. K., & Chen, R. (2021). GRP78 facilitates M2 macrophage polarization and tumour progression. Cellular and Molecular Life Sciences, 78(23), 7709–7732.
Zhang, Y., Cheng, R., Ding, T., & Wu, J. (2024). Discrepancies in PD-L1 expression, lymphocyte infiltration, and tumor mutational burden in non-small cell lung cancer and matched brain metastases. Translational Lung Cancer Research, 13(12), 3590–3602.